Genetic differentiation and intrinsic genomic features explain variation in recombination hotspots among cocoa tree populations

Enrique J. Schwarzkopf[1], Juan C. Motamayor[2], and Omar E. Cornejo[1,*]

[1]School of Biological Sciences, Washington State University, 100 Dairy Road, Pullman, WA 99164, USA

[2]Universal Genetic Solutions, LLC

[*]Corresponding author: ocornejo@gmail.com

November 29, 2018

Abstract

Our study investigates the possible drivers of recombination hotspots in *Theobroma cacao* using ten recently diverged populations. This constitutes the first time that recombination rates from more than two populations of the same species have been compared, providing a novel view of recombination at the population-divergence time-scale. For each population, a fine-scale recombination map was generated using a method based on linkage disequilibrium (LD). They revealed higher recombination rates in a domesticated population and a population that has undergone a recent bottleneck. We address whether the pattern of recombination rate variation along the chromosome is sensitive to the uncertainty in the per-site estimates. We find that uncertainty, as assessed from the Markov chain Monte Carlo iterations is orders of magnitude smaller than the scale of variation of the recombination rates genome-wide. We inferred hotspots of recombination for each population and find that the genomic locations of these hotspots correlate with genetic divergence between populations (F_{ST}). The large majority of inferred hotspots are not shared between populations (55.5%). We developed novel randomization approaches for the generation of appropriate null models to understand the association between hotspots of recombination and both DNA sequence motifs and genomic features. Hotspot regions contained fewer known retroelement sequences than expected, and were overrepresented near transcription start and termination sites. Indicating that recombination hotspots are evolving in a way that is consistent with genetic divergence, but are also preferentially driven to regions of the genome that contain specific features.

Introduction

Genetic variation is fundamental for evolutionary forces like selection and genetic drift to act. Selection and drift also contribute to a loss of variation, which means that they must act in tandem with forces that maintain variation along the genome in order for populations to continue evolving over prolonged periods of time. Selection and drift also contribute to a loss of variation, which means that they must act in tandem with forces that maintain variation along the genome in order for populations to continue evolving over prolonged periods of time. Recombination's rearranging of genetic material onto different backgrounds generates a larger set of haplotype combinations on which selection can act, reducing the magnitude of Hill-Robertson interference (Felsenstein, 1974). Different regimes of recombination can strongly influence how efficient selection is at purging deleterious mutations and increasing the frequency of beneficial mutations in the population (Felsenstein, 1974).

Genome-wide fine-scale recombination maps can help elucidate the distribution of recombination events along the genome (Myers et al., 2005; Auton et al., 2012; Brunschwig et al., 2012; Paape et al., 2012; Choi et al., 2013; Hellsten et al., 2013; Singhal et al., 2015; Stevison et al., 2016). These maps are constructed using methods that use the coalescent to leverage current patterns of LD in order to estimate historical rates of recombination between sites along the genome (Auton and McVean, 2007). Studies in a wide range of species have shown that recombination rates are not uniform along the genome and general patterns of variation have been described (Begun and Aquadro, 1992; Akhunov et al., 2003; Wu et al., 2003; Anderson et al., 2004; McVean et al., 2004; Mézard, 2006; Kim et al., 2007; Gore et al., 2009; Schnable et al., 2009; Branca et al., 2011; Paape et al., 2012). One of these patterns is the reduced recombination rate in centromeric regions of the chromosomes and the progressive increase of recombination rates as the physical distance to telomeres decreases (Begun and Aquadro, 1992; Akhunov et al., 2003; Wu et al., 2003; Anderson et al., 2004; Gore et al., 2009;

Schnable et al., 2009). Another, perhaps more interesting pattern that has been observed is regions with unusually high rates of recombination spread throughout chromosomes: recombination hotspots (McVean et al., 2004; Brunschwig et al., 2012; Paape et al., 2012; Hellsten et al., 2013; Stevison et al., 2016; Shanfelter et al., 2018). The importance of recombination hotspots lies in their ability to shuffle genetic variation at higher rates than the rest of the genome, profoundly impacting the dynamics of selection for or against specific mutations (Felsenstein, 1974).

A variety of genomic features have been identified as being associated with regions of high recombination. In *Arabidopsis thaliana*, *Taeniopygia guttata*, *Poephila acuticauda*, and humans, hotspots have been linked to transcriptional start sites (TSSs) and transcriptional termination sites (TTSs) (Myers et al., 2005; Choi et al., 2013; Singhal et al., 2015). In *Mimulus guttatus* hotspots were found to be associated with CpG islands (short segments of cytosine and guanine rich DNA, associated with promoter regions) (Hellsten et al., 2013). These patterns point to recombination occurring frequently near, but not within coding regions. The formation of chiasmata is important for the proper disjunction of chromosomes during meiosis (Martinez-perez et al., 2008), but repeated double-strand breaks can lead to an increased mutation rate (Rodgers and Mcvey, 2015). In coding regions in particular this excess mutation rate can have a high evolutionary cost, due to the likelihood of deleterious mutations arising being higher than that of beneficial ones (Haldane, 1937; Crow, 1970; Wloch et al., 2001; Sanjuán et al., 2004; Eyre-Walker and Keightley, 2007). Recombination hotspots have also been found to be correlated with particular DNA sequence motifs. In some mammals, including *Mus musculus* (Brunschwig et al., 2012) and apes (Auton et al., 2012; Stevison et al., 2016) binding sites for PRDM9, a histone trimethylase with a DNA zinc-finger binding domain, have been found to correlate with recombination hotspots. In *Arabidopsis*, proteins have been identified that limit overall recombination rate, leading to an increased recombination rate genome-wide in mutants (Fernandes et al., 2018). However,

these proteins have not been shown to direct recombination to particular regions, and are therefore not expected to affect the location of recombination hotspots.

Recent work on recombination in apes (Stevison et al., 2016) found little correlation of recombination rates in orthologous hotspot regions when looking between species, but a strong correlation when comparing between two populations of the same species. This suggests that recombination hotspots are potentially changing in ways that match demographic patterns, differentiating at a similar rate as genomic sequences. The identification of ten recently diverged populations of the cocoa tree, *Theobroma cacao* (Motamayor et al., 2008; Cornejo et al., 2018) can be leveraged to study short-term drivers of recombination hotspots. These ten populations originate from different regions of South and Central America, and include one fully domesticated species (Criollo), used in the production of fine chocolate, and nine wilder, more resilient species which generate higher cocoa yield than the Criollo variety (fig. 1) (Motamayor et al., 2008; Henderson et al., 2007; Cornejo et al., 2018). These ten populations have been shown to be highly differentiated and the history of diversification has been recently confirmed using genomic data (Cornejo et al., 2018). Comparing the locations of hotspots between these ten populations of *T. cacao* can contribute to the understanding of hotstpot turnover in short periods of time among highly differentiated populations. These comparisons also contribute to our understanding of how demographics impact the turnover of recombination hotspot locations.

Fine-scale, LD-based recombination maps have been constructed for a number of plant models (Paape et al., 2012; Choi et al., 2013; Hellsten et al., 2013), and in all of them a variety of correlates of recombination rate have been identified. Unlike these model plants with short generation times, *T. cacao* is a perennial woody plant with a five-year generation time (Henderson et al., 2007). Studying recombination in *T. cacao* presents particular difficulties due to its long generation time, making it difficult to directly measure rates of recombination. However, linkage-based methods allow for the estimation of historic recombi-

nation rates (Auton and McVean, 2007), facilitating the study of historical recombination in *T. cacao*. Theoretical studies have shown that population structure can generate artificially inflated measures of LD (Ohta, 1982; Li and Nei, 1974), which would be detrimental to our estimates of recombination. For this reason recombination maps were constructed independently for each population. In contrast to previous studies, which have focused primarily on recombination rates, this study attempts to describe the relationship between recombination hotspots and a variety of factors.

A series of questions were addressed in this work: (i) How are recombination rates distributed within 10 highly differentiated populations of *T. cacao*, and how do they compare to each other? (ii) How are hotspots distributed along the genome of each of the ten populations of *T. cacao*, and can these distributions be explained by patterns of population genetic differentiation? (iii) Are there identifiable DNA sequence motifs that are associated with the location of recombination hotspots along the *T. cacao* genome? (iv) Are there genomic features (e.g. TSSs, TTSs, exons, introns) consistently associated with recombination hotspot locations across *T. cacao* populations?

In order to address these questions, we used an LD-based method to estimate recombination rates, since *T. cacao*'s generation time and sheer size make performing a large number of backcrosses unfeasible. We used the estimated recombination rates in a maximum likelihood statistical framework to infer the location of recombination hotspots. Then we compared the location of hotspots across populations and found evidence that, while hotspots generally follow patterns of genetic differentiation, their turnover rate is faster than the rate of divergence. We used resampling schemes to generate null assumptions for the content of known DNA sequence motifs in ubiquitous recombination hotspots, as well as the overlap of population recombination hotspots with genomic traits. The resampling schemes used to identify these associations are novel in the context of this work and were designed to take into account the size and distribution of elements in the genome. Our findings suggest that

recombination hotspot locations generally follow patterns of diversification between populations, while also having a strong tendency to occur close to TSSs and TTSs. Moreover, we find a strong negative association between the occurrence of recombination hotspots and the presence of retroelements.

Results

Comparing recombination rates between populations

Populations show a mean recombination rate r/kb between 2.1×10^{-5} and 5.25×10^{-3} (table 1), with a long-right-tailed distribution (fig. 3). The extreme recombination rate values affect the mean, driving it to values consistently higher than the median. The pattern of recombination rates along the genome varied between populations, as can be seen in the comparison of the Nanay and Purus third chromosome (fig. 4). The median 95% probability interval for recombination rate across the genome for each population was found to be several orders of magnitude larger than the uncertainty per site, estimated as the median 95% Credibility Interval of the trace for each position in the genome for that population (table 6).

Overall, the recombination rate for most of the populations was higher than estimated mutation rates for multicellular eukaryotes of 10^{-6} changes per kb per generation (Lynch, 2010; Exposito-Alonso et al., 2018) (table 1). Two populations, Guianna and Criollo, were notable exceptions, having higher average recombination rates than the other populations by one and two orders of magnitude respectively. Guianna and Criollo also had a lower effective population size (N_e) (Cornejo et al., 2018) by one and two orders of magnitude respectively. However, there was no significant linear trend between mean N_e and r/kb

(p=0.09045), indicating that, for a high enough N_e, the ability to detect recombination events is not dictated by the effective population size. When Criollo and Guianna were excluded, the relationship was also not present ($p = 0.6544$). When all populations were included, the inbreeding coefficient (F) showed no significant linear association with mean r/kb ($p = 0.3361$). The average recombination rate per population was transformed from r/kb to cM/Mb (table 1). The average cM/Mb was 4.6×10^{-04}.

In order to compare the average recombination rates of the different populations, a Kruskal-Wallis test was performed for every pair of populations. The only pair of populations that did not show a significant difference in mean recombination rate was the pair of Nacional and Nanay ($p = 0.3$). All other pairwise comparisons were highly significant ($p < 2 \times 10^{16}$).

Comparing recombination hotspot locations between populations

The majority (55.5%) of hotspots identified were not shared between populations. The 25 most numerous sets of hotspots are represented in fig. 6. The nine largest of these are sets of hotspots unique to a single population. The hotspots unique to the remaining population (Criollo) formed the eleventh largest set.

The recombination rate in hotspot regions for nine of the populations was on average between 22 and 237% higher than the average recombination rate of the genome. The exception was Guianna, which only showed an approximately 1% increase in average recombination rate in hotspots regions when compared to that of the non-hotspot regions.

Despite the majority of hotspots not being shared between populations, pairwise Fisher's exact tests between populations indicated significantly more overlap than expected (if hotspots were randomly distributed along the genome) between hotspots for most pairs of populations (table 2). There were three comparisons that did not show significantly more overlap

than expected: Amelonado-Nacional, Amelonado-Purus, and Criollo-Nacional. A Mantel test comparing distances between populations based on shared hotspots and F_{ST} values between populations resulted in a significant correlation between them ($r = 0.66$, $p = 0.002$). The correlation between eigenvectors from a correlation matrix and those of the genetic covariance matrix were also explored. When all populations were included, we found that the first eigenvector from the genetic covariance matrix was not significantly correlated with the first eigenvector from the hotspot correlation matrix ($p = 0.7055$), but the second genetic eigenvector was ($p = 0.009007$, $r = 0.7711638$). However, the first eigenvector of the genetic covariance matrix captured the difference between the Criollo population (the only domesticated variety) and the rest of the populations. The second eigenvector explains most of the natural differentiation across populations (Cornejo et al., 2018). For that reason, we decided to exclude Criollo and repeat the analysis. We found that the first eigenvector from the correlation matrix constructed from shared hotspot information was not significantly correlated with either of the first two eigenvectors of the genetic covariance matrix when Criollo was excluded (eigenvector 1: $p = 0.1314$, eigenvector2: $p = 0.3376$).

To study the effects of demographic history more closely, shared hotspots were converted to dimensions of a multiple correspondence analysis and modeled along a previously constructed drift tree (Cornejo et al., 2018). The model assuming an OU process (stabilizing selection) is consistent with a higher trait maintenance than the model assuming Brownian motion (drift). Modeling the dimension as a Brownian motion was a better fit (AIC=79.4) than modeling it as an Ornstein-Uhlenbeck (OU) process (AIC=81.4), which is consistent with the small number of hotspots shared between populations.

Identifying DNA sequence motifs associated with the locations of recombination hotspots

RepeatMasker was used to analyze the set of recombination hotspots that were present

in at least eight *T. cacao* populations (17 total hotspots), as well as the consensus set of recombination hotstpots, and the reference genome. In order to determine whether a particular set of DNA sequence repeats was overrepresented in the regions of ubiquitous recombination hotspots, the percentage of DNA sequence that was identified as potentially being from retroelements or DNA transposon was compared to an empirical distribution. The percentage of observations from the distribution which were greater than the observed are reported in table 3. While retroelements were found to be underrepresented in the ubiquitous hotspots, DNA transposons were marginally overrepresented.

Identifying genomic features associated with the location of recombination hotspots

An overrepresentation of recombination hotspots was found in all ten of the populations at transcriptional start sites (TSSs) and transcriptional termination sites (TTSs)(table 4). The level of overrepresentation of hotstpots in particular regions was compared to a null expectation based on simulations of hotspots of the same size as the ones detected distributed randomly along chromosomes. For all populations, all 1000 simulations showed a lower proportion of overlap with TSSs and TTSs than the observed overlap. In the case of exons and introns, seven populations (Contamana, Criollo, Iquitos, Maranon, Nacional, Nanay, Purus) had an observed value that was lower than all, or almost all (Purus for exons), simulations. Three of the remaining four populations (Amelonado, Curaray, and Nanay) had no clear trend in either direction (table 2). The final population (Guianna) showed an overrepresentation of hotspots in both exons and introns.

Discussion

Understanding how recombination rates vary between recently diverged populations is an important step toward disentangling the role of recombination in genetic differentiation. This set of *T. cacao* populations presents a unique opportunity to observe recombination in long-established, non-domesticated populations, as well as a recently established non-domesticated population (Guianna) and a domesticated population (Criollo) (Cornejo et al., 2018; Bartley, 2005). This model has allowed us to explore divergence patterns of recombination hotspot at a scale bellow that of species divergence. Our results point to a conservation of hotspots between populations that generally mirrors the patterns of genetic differentiation between populations. However, we find that the correlation between genetic differentiation and shared hotspots does not fully explain the observed hotspots, in part due to the majority of hotspots being found in a single population. We find that TSSs and TTSs are strongly associated with recombination hotspots in all populations, which is consistent with previous findings in plants (Paape et al., 2012; Choi et al., 2013; Hellsten et al., 2013). This factor seems to play an important role in determining the location of novel hotspots. Finally, hotspots that are shared by at least eight populations appear to be associated with DNA transposons, pointing to a potential mechanism for the maintenance of recombination hotspots at the population-divergence time-scale.

Comparing recombination rates between populations

We found that the eight long-established, non-domesticated *T. cacao* populations show a recombination rate (r/kb) lower than multicellular eukaryotic mutation rates (table 1), while the other two populations (Criollo and Guianna) show unusually high average recombination rates in comparison. For all populations, the mean recombination rate was found to be lower

than the median. This is consistent with high rate outlier values; an expected result in the presence of recombination hotspots. Using the effective population size for *Medicago truncatula* from Siol et al. (2007) and the estimate of *rho* from Paape et al. (2012), we calculated r/kb ($= 4 \times 10^{-3}$) and found that it was comparable with the rate found for the Criollo population (table 1). We also calculated the median recombination rate in cM/Mb for each chromosome using the Kosambi mapping function (Kosambi, 1943) over non-overlapping, 100 SNP windows. The average cM/Mb for all populations was 4.6×10^{-04}, which is lower than has been measured for any Malvale (Kundu et al., 2015), but not as low as the lowest measured for conifers (Chen et al., 2010; Stapley et al., 2017). Average recombination rates in cM/Mb varied between populations from Amelonado (4.04×10^{-06}) to Criollo ($3.91 \times ^{-03}$). Previous work (Cornejo et al., 2018) has shown that Criollo is the only population showing a strong signature of domestication, as revealed by much higher drift than that observed for other populations. Domestication has been observed to increase recombination rates, particularly in plants (Ross-Ibarra, 2004), and is a possible explanation for the higher recombination rate observed for the Criollo population. The high recombination rate observed in Guianna can be explained in a similar way; while Guianna does not show a strong signature of domestication, it is the most recently established population (Bartley, 2005), and it has also undergone a recent bottleneck (Cornejo et al., 2018). It's possible that the Guianna population is undergoing the initial stages of domestication and its increased recombination is an early indicator of this. It is possible that the high recombination rates estimated for Criollo and Guianna can be explained by biases in estimation caused by errors associated to small samples or low genetic variation; yet, the recombination rates for Amelonado (another population with low variation) or Purus (a population with small sample size) did not present this problem. Analyses exploring mutations of putative recombination suppression genes (Fernandes et al., 2018) could help disentangle the nature of this extreme variation in recombination rate in the Criollo and Guianna populations.

Despite recombination rates for eight of the ten populations being of the same order of magnitude, pairwise comparisons of average rates indicated that most populations have a significantly different rate of recombination from the others. The only exception were Nacional and Nanay whose average rates were not significantly different from each other. These two populations, however, are not more closely related to each other than they are to other populations, based on sequence divergence (Cornejo et al., 2018). We interpret this result as suggestive that their similarity is not due to genetic similarity, but some other factors, e.g. epigenetics.

The likelihood of detecting Hotspots of recombination in the genome will likely be affected by the amount uncertainty in the estimates of recombination site-wise and region-wise. Yet, we have been unable to identify any study where the magnitude of the uncertainty in the estimates of recombination are assessed to address this issue. We have performed careful comparisons and assessed the magnitude of the uncertainty in the estimation of recombination rates to show that this uncertainty is several orders of magnitude smaller than the variation in recombination rates across the genome (table 6). If the length of the chains had been maintained at 40MM generations, this would have increased the uncertainty in local estimates making our assessment of rate variation along the genome more challenging.

Comparing recombination hotspot locations between populations

Similarly to recombination rates, the location of recombination hotspots can be very informative to questions of divergence between populations. Understanding the pattern and rate of change of recombination hotspots at the population level can elucidate their role in shaping genome architecture, impacting how effectively selection operates(Felsenstein, 1974). We found that a large proportion (55.5%) of hotspots are unique to a single population, which can be seen as an indicator that the turnover rate for hotspots is faster than the time it took

the 10 populations to diverge. This variability of hotspot location between populations points to demographic history not being the main driver of recombination hotspot location. However, the hotspots tend to appear in similar regions, as demonstrated by the Fisher's exact tests (table 2). This dichotomy can be explained by considering that the proportion of the genome occupied by recombination hotspots is very low, so even a small proportion of hotspots from two different populations being in the same region is enough for the Fisher's exact test to recognize them as significantly similar. This small but significant similarity can occur by recombination being limited in its possible positioning along the genome, but not to the point of forcing hotspots to occur consistently in the same locations, and thus maintaining some level of stochasticity.

Given the significant proportion of overlapping hotspots between populations, it was still important to explore whether the similarities can be explained by shared genetic history. If demographic history explained the evolution of hotspot location, it would be expected that more closely related populations would have a higher percent of overlapped hotspots. A significant relationship was found between population differentiation (F_{ST}) and the differentiation between populations based on shared hotspots (Mantel test, $r = 0.66$, $p = 0.002$). The comparison between the hotspot correlation matrix and the genetic covariance matrix supports what was found when comparing the hotspot correlation matrix to the F_{ST} matrix. One caveat is that the first genetic eigenvector, which separated Criollo from the other populations, was not correlated with the first hotspot correlation eigenvector, indicating that Criollo's domestication generated a genetic pattern that deviates from the pattern of shared hotspots. This indicates that, to some extent, the genetic differentiation and the location of hotspots are mirroring each other, which could be due to recombination hotspots being a product of the shared history between the populations. However, since recombination rates were estimated using a coalescent-based method, we expect historical relationships to be represented in our findings. We also transformed the information of hotspot overlap to allow

for the modeling of hotspots as traits along a population tree. Our results, showing that a Brownian motion model (AIC=79.4) better fits the data than a model with stabilizing selection Ornstein-Uhlenbeck model (AIC=81.4), suggests in first principle that drift alone could explain the evolution of the location of recombination hotspots. However, the absolute number of hotspots that are shared among populations indicates that demographic history alone is insufficient to explain the evolution of recombination hotspots in this species. Previous studies looking at apes and finches have explored recombination hotspots in multiple species and as many as two populations of the same species (Singhal et al., 2015; Stevison et al., 2016; Shanfelter et al., 2018), but this study is the first to compare more than two populations of the same species at once. The increased number of populations allows us to analyze the relationship between population genetic processes and recombination. Our results suggest that the pattern of gains and losses of recombination hotspots can be very dynamic and the landscape of recombination changes rapidly during the process of diversification within a species. This dynamism can have a tremendous impact on the adaptive dynamics of a species, and it should be taken into account, considering that theoretical studies tend to assume that recombination rates are constant during the evolution of populations (Hudson and Kaplan, 1988; Donnelly and Kurtz, 1999).

One conclusion that follows from these results is that, while shared recombination hotspots can to some extent be explained by patterns of genetic differentiation, some of the sharing can simply be due to a tendency for hotspots to arise in similar locations. It has been observed in other organisms that hotspots of recombination are frequently associated to specific genomic features (including TSSs and TTSs) (Auton et al., 2013; Choi et al., 2013; Hellsten et al., 2013; Myers et al., 2005; Singhal et al., 2015) or DNA sequence motifs (Auton et al., 2012; Brunschwig et al., 2012; Stevison et al., 2016). These factors can affect the landscape of recombination, generating the patterns of shared hotspot locations between populations that we are observing in *T. cacao*.

362

363 *Identifying DNA sequence motifs associated with the locations of recombination hotspots*

364

365 The analysis of 17 hotspots shared between at least eight populations of *T. cacao* found
366 an underrepresentation of retroelements and a marginal overrepresentation of DNA trans-
367 posons when compared to the entire genome. These results are not entirely surprising as
368 it has been already suggested that transposable elements (TEs) tend to be enriched in ar-
369 eas of low recombination in *Drosophila* as a consequence of selection against TEs (Rizzon
370 et al., 2002). The marginal over-representation of DNA transposons in the most conserved
371 recombination hostspot is unexpected, given that all previous observations have shown a
372 reduced representation of mobile elements in areas with high recombination rate (Rizzon
373 et al., 2002). It's possible that DNA transposons are, at least in part, responsible for the
374 maintenance of recombination hotspots as populations diverge, from which we expect that
375 site-directed recombination is more frequent in these locations of the genome. However, the
376 low percentage of these sequences observed in the set of all hotspots (table 3) indicates that
377 these sequences only have a small effect on the maintenance of hotspots. It has been observed
378 in humans that short DNA motifs enriched for repeat sequences determine the location of 40
379 per cent of hotspots enriched for recurrent non-allelic homologous recombination (Mcvean,
380 2010). One potential explanation that for why natural selection does not eliminate hotspots
381 in these regions is the possibility that these regions don't produce a large enough mutational
382 load for natural selection to remove them from the population (Mcvean, 2010).

383

384 *Identifying genomic features associated with the location of recombination hotspots*

385

386 For all ten populations, an overrepresentation of hotspots was found in the areas imme-
387 diately preceding and following transcribed regions of the chromosome. This matches the

findings of previous studies in *Arabidopsis thaliana* (Choi et al., 2013), *Taenipygia guttata* and *Poephila acuticauda* (Singhal et al., 2015), and humans (Myers et al., 2005). The most likely explanation is that recombination events within genes are selected against. The rationale is that a recombinant chromosome that is split in the middle of a coding region will have a higher risk of being inviable, and therefore not represented in the current set of chromosomes for its population. Recombination occurring in transcription start and stop sites, on the other hand, does a much better job at breaking up haplotypes, while preserving the functionality of coding regions. This rational is supported by previous findings of increased recombination rates in these regions (Choi et al., 2013). It's also supported by results from PRDM9 knock-out *Mus musculus*, which has shown a reversion to hotspots located near TSSs (Brick Kevin et al., 2012). The enrichment of *T. cacao* hotspots in TSSs and TTSs is thus a reasonable result given that zinc-finger binding motifs and potential modifiers like PRDM9 have not been identified in the species.

Implications for the evolutionary history of T. cacao

Overall, our results show a large consistent pattern where recombination rates in *T. cacao* are of the same magnitude as mutation rates, but show a high diversity in location and number of hotspots of recombination that cannot be explained solely by the process of diversification of the populations. In fact, the results are indicative that the turnover rate of hotspots is faster than the process of divergence among populations. A potential hypothesis that could explain the rapid turnover of hotspots of recombination and the relative differences in recombination among populations is that epigenetic changes control the turnover of recombination in plants. This hypothesis is not unreasonable given the recent observation of epigenetic control of recombination in plants (Yelina et al., 2015). Further theoretical and simulation work should be done in order to better understand the implications of the

rapidly changing recombination hotspots in adaptive dynamics. We also show that there is an overall underrepresentation of hotspots in exons and introns for most populations, which is consistent with purifying selection acting against changes that could result in disruptions of gene function. On the other hand, we observed an overrepresentation of hotspots in TTSs and TSSs for all ten populations. This could impact the maintenance and spread of beneficial traits in the population by shuffling allelic variants of genes without causing disruption of their function. We hypothesize that the enrichment of hotspots of recombination in TTSs and TSSs can have an important impact in the spread of beneficial mutations across different genomic backgrounds; increasing the rate of adaptation to selective pressures (e.g. selection for improved pathogen response).

Materials and Methods

Comparing recombination rates between populations

Sequence data were downloaded from the Cacao Genome Database and NCBI (Accession PRJNA488484), including the reference sequence for each chromosome and the full genome annotation (*Theobroma cacao* cv. Matina 1-6 v1.1)(Motamayor et al., 2013). Processing was done using the pipeline from (Cornejo et al., 2018) available at the github repository *oeco*28/*Cacao_Genomics*. Full genome data was used from a total of 73 individuals across 10 populations (Cornejo et al., 2018): Criollo (N = 4, #SNPs = 309,818), Curaray (N = 5, #SNPs = 1,106,871), Contamana (N = 9, #SNPs = 2,097,618), Amelonado (N = 11, #SNPs = 373,789), Maranon (N = 14, #SNPs = 1,783,226), Guianna (N = 9, #SNPs = 770,729), Iquitos (N = 7, #SNPs = 1,575,711), Purus (N = 6, #SNPs = 1,184,181), Nanay (N = 10, #SNPs = 830,885), and Nacional (N = 4, #SNPs = 718,099). VCFTools (Danecek

Petr et al., 2011) was used to remove all singletons and doubletons. Only bi-allelic single nucleotide polymorphisms (SNPs) were retained and were exported in LDhat format.

In order to estimate recombination rates we used the *interval* routine of LDhat (Auton and McVean, 2007), a program that implements coalescent resampling methods to estimate historical recombination rates from SNP data. To reduce computation time, each chromosome was split into windows, each containing 2000 SNPs. To counteract the overestimation of recombination rate produced at the ends of the windows, an overlap of 500 SNPs was left between consecutive windows. The final window for each chromosome did not always match the general scheme, so the final 2000 SNPs were taken (making the overlap with the second to last window variable, but never less than 500 SNPs) (fig. 2). Once these windows were generated, LDhat was run over each window with 100 million iterations, sampling every 10 thousand iterations (10,000 total points sampled), with a block penalty of 5. Lookup tables with a grid of 100 points, a population mutation rate parameter (θ) of 0.1 and a number of sequences (n) of 50 were used for all populations. The first 50 million iterations were discarded as burn-in. Once recombination rates were calculated, 250 positions were cut off from both windows involved in each overlap, so that the estimates for the first half of the overlap was taken from the end of the preceding window and the estimates for the second half of the overlap were taken from the beginning of the following window. The final overlap in each chromosome was split in order to take only 250 SNPs from the second to last window, regardless of the remaining size of the last window. The remaining rate estimates were then merged in order to obtain the recombination rates for the entire chromosome. This was done for each chromosome of each population.

The estimation of recombination rates with LDhat is approximated using a sampling scheme with a Markov Chain Monte Carlo (MCMC) algorithm as implemented in the *interval* routine. The inference of recombination rates is the result of the integration of estimated parameter values across iterations with the routine *stats*. In the majority of recent studies

where LDhat or LDhelmet are used (Myers et al., 2005; Auton et al., 2012; Brunschwig et al., 2012; Paape et al., 2012; Auton et al., 2013; Choi et al., 2013; Singhal et al., 2015; Stevison et al., 2016), whether there is convergence of the Markov chains has not been explicitly investigated. One study that we're aware of has used simulations to asses whether their small sample size affected their ability to obtain reliable estimates of recombination using LDhelmet (Booker et al., 2017), but did not assess the uncertainty of the estimates from the MCMC process itself. We argue that evaluation of convergence is important to assess the confidence in the estimated reported values, especially if there is interest in analyzing the differences in recombination rate along the genome. Visual inspection of pilot runs of the analysis demonstrated that convergence was not achieved after running 40M iterations, which is why the length of the chains was increased to 100M iterations. Additionally we explored the uncertainty in the estimates of recombination site-wise by integrating over the trace of the estimates for recombination rate to infer the 95% Credibility Interval. We then estimated the 95% of recombination estimates range across all sites in the genome to have an overall measure of uncertainty that we compared to the median 95% Credibility Interval for the trace of each position.

In order to compare recombination rates, the effective population size (N_e) calculated for each population (Cornejo et al., 2018) was used to convert rates in $N_e r/kb$ to r/kb. Differences in the mean genome-wide recombination rate between populations were then tested using the Kruskal-Wallis test, using the `kruskal.test` function from the `stats` package in `R` (R Core Team, 2018). There were 45 comparisons, making the Bonferroni correction cutoff value: $\alpha = 0.0011$. To transform per population recombination rates from r/kb to cM/Mb, we divided each chromosome into windows of 100 SNPs and used the Kosambi mapping function (Kosambi, 1943). The median for the windows of a chromosome was then calculated, and the average of each population's chromosomes was taken as that population's average recombination rate in cM/Mb.

Comparing recombination hotspot locations between populations

Recombination hotspots were estimated with LDhot (Auton and McVean, 2007), a likelihood-based program that tests whether a single distribution model or a two distribution model better explains the observed recombination rates in 1 kb sliding windows (default), for each chromosome. Each chromosome was run in its entirety, with the number of simulations (nsims) set to 1000. The resulting potential hotspots were refined by an alpha of 0.001, and overlapping hotspots were merged.

To determine the set of consensus hotspots, the hotspots from all populations were merged. Two hotspots from different populations were considered to be shared if they both overlapped with the same hotspot in the consensus set. To summarize all shared hotspots, a Boolean matrix was constructed, in which a population having a hotspot that overlaps with a hotspot in the consensus list leads to an indication of presence of the consensus hotspot in that population. This matrix was used to determine hotspots shared by two or more populations.

A Fisher's exact test was run for each pair of populations in order to determine whether hotspots for the pair of populations overlap significantly more than expected. The BED files containing the location of the recombination hotspots for each pair of populations were compared using Bedtools:fisher (Quinlan and Hall, 2010). The number of comparisons was 45, making the the Bonferroni correction cutoff value: $\alpha = 0.0011$.

In order to compare the relationships between populations based on shared hotspots we calculated Jaccard distances (`distance` function, `philentropy` package, `R`) (Drost, 2018) and compared them to a published F_{ST} matrix (Cornejo et al., 2018) using a Mantel test (`mantel.rtest` function, `ade4` package, `R`) (Chessel et al., 2004; Dray and Dufour, 2007; Dray et al., 2007; Bougeard and Dray, 2018).

The Boolean matrix for shared hotspots was also used to explore the relationship between hotspot similarities and genetic covariances from a previous study (Cornejo et al., 2018). Singletons were removed from the hotspot matrix, which was converted to a correlation matrix using the `mixed.cor` function from the `psych` package in `R` (Revelle, 2018). The `mixed.cor` function was used due to its ability to calculate Pearson correlations from dichotomous data. We then used the `eigen` function in `R` (R Core Team, 2018) to generate eigenvectors for the hotspot correlation matrix and the genetic covariance matrix. Pearson correlations between the first and second eigenvector of the genetic covariance matrix and the hotspot correlation matrix were then calculated (`cor.test` function, `stats` package, `R`)(R Core Team, 2018). This analysis was done once with all populations included, and once with the Criollo population excluded before correlations were calculated.

In order to model the presence or absence of hotspots along a drift tree, a multiple correspondance analysis was used on the Boolean matrix of shared hotspots using the `MCA` function from the `FactoMineR` package in `R` Lê et al. (2008). Nine dimensions were retained and used as traits along a previously generated drift tree (Cornejo et al., 2018). Using the `Rphylopars` package in `R` (Goolsby et al., 2016), the dimensions were modeled as Brownian motion and as an Ornstein–Uhlenbeck process. The fit of the two models were compared using the AIC values for the best fitting models of each type.

Identifying DNA sequence motifs associated with the locations of recombination hotspots

Motifs associated with hotspots were found using RepeatMasker (Smith et al., 2016). The entire genome, the set of consensus hotspots, and a set of ubiquitous hotspots (hotspots shared by at least eight of the populations) were examined with RepeatMasker, using normal speed and "theobroma cacao" in the species option. In order to determine whether ubiquitous hotspots were enriched for particular DNA sequences, a set of the same number and size

of sequences was randomly selected from the genome using Bedtools:shuffle (Quinlan and Hall, 2010) and examined with RepeatMasker. This simulation was repeated one thousand times and a null distribution against which observed values were compared was constructed from the results.

Identifying genomic features associated with the location of recombination hotspots

Testing whether recombination hotspots were overrepresented near particular genomic features was done by using a resampling scheme to establish null expectations and then comparing the observed value to the empirical distribution. For each feature, locations were retrieved and the number of observed hotspots that overlap with this feature were counted. To determine whether this amount of overlapping hotspots was unusually high or low, a set of hotspots that matched the number of hotspots and the size of each hotspot was simulated. These simulated hotspots were placed randomly along the chromosome, using a uniform distribution. The simulation was run 1000 times and the number of simulated hotspots that overlap with the true genomic features was measured for each simulation. The simulations generate an expected distribution of overlap with the genomic feature, and the true value was then compared to the distribution. When simulated hotspots overlapped, the location of one of them was sampled again. Features tested were: Transcriptional start sites (TSSs), transcriptional termination sites (TTSs), exons, and introns. TSSs and TTSs are considered to be the 500bp upstream and downstream of coding regions respectively.

The reason for the proposed novel resampling scheme is that, if the size and distribution of genomic features and hotspots were not taken into account, it would set unrealistic expectations for the overlap between features under a null model of no association. In this sense, the null model would be inappropriate and potentially inflate the false positive rate.

568 *Data and code availability*

569

570 Rate and summary files from LDhat runs as well as hotspots for each population will be
571 placed in a Dryad repository (url). Scripts for LDhat and LDhot runs as well as additional
572 analysis is compiled in the following github repository $ejschwarzkopf/recombination-map$.

573

Tables

Population	Mean 4Ner/kb	Mean Ne	Mean r/kb	Median r/kb	Lower Bound (Mean r/kb)	Upper Bound (Mean r/kb)	Mean cM/Mb
Amelonado	1.58	15744	2.51e-05	2.40e-09	2.48e-05	2.54e-05	4.04e-06
Contamana	8.53	61102	3.49e-05	4.92e-06	3.48e-05	3.50e-05	7.74e-05
Criollo	14.60	695	5.25e-03	4.27e-03	5.23e-03	5.27e-03	3.91e-03
Curaray	10.36	58213	4.45e-05	1.78e-05	4.44e-05	4.46e-05	1.18e-04
Guianna	8.66	4651	4.65e-04	7.74e-06	4.63e-04	4.67e-04	2.74e-04
Iquitos	4.23	49984	2.11e-05	5.88e-09	2.10e-05	2.12e-05	1.84e-05
Maranon	4.09	34037	3.01e-05	1.64e-08	2.99e-05	3.02e-05	1.68e-05
Nacional	4.66	26060	4.47e-05	9.76e-08	4.44e-05	4.49e-05	4.10e-05
Nanay	6.82	42429	4.02e-05	1.51e-07	4.00e-05	4.04e-05	1.33e-05
Purus	5.95	17357	8.57e-05	7.74e-06	8.54e-05	8.60e-05	1.23e-04

Table 1: Recombination rates in $4N_e r/kb$, r/kb, and cM/Mb for all ten *T. cacao* populations. The N_e that was used for the transformation is also reported for each population, as are the lower and upper bounds of a 95% confidence interval for r/kb.

Population	Ame	Con	Cri	Cur	Gui	Iqu	Mar	Nac	Nan
Amelonado	-	-	-	-	-	-	-	-	-
Contamana	<2e-07	-	-	-	-	-	-	-	-
Criollo	<9e-05	<5e-13	-	-	-	-	-	-	-
Curaray	<3e-05	<3e-37	<5e-08	-	-	-	-	-	-
Guianna	<3e-06	<1e-37	<7e-07	<4e-20	-	-	-	-	-
Iquitos	<4e-08	<6e-87	<2e-11	<3e-16	<2e-29	-	-	-	-
Maranon	<6e-13	<7e-77	<2e-11	<2e-20	<5e-33	<4e-64	-	-	-
Nacional	0.0015	<2e-43	0.0212	<7e-14	<3e-06	<6e-14	<3e-13	-	-
Nanay	0.0004	<2e-44	<9e-11	<4e-16	<2e-21	<3e-39	<2e-38	<9e-06	-
Purus	0.1782	<4e-117	<2e-05	<2e-29	<1e-33	<2e-39	<8e-43	<6e-27	<2e-21

Table 2: Fisher's exact test p-values for pairwise comparisons of recombination hotspot locations between populations of *T. cacao*

Measures	Observed % ubiquitous HS	Observed % all HS	Observed % whole genome	Mean % Sim	% Sim >ubiquitous HS
Retroelements	2.34	9.45	11.12	11.11	99.9
DNA transposons	1.94	1.64	1.10	1.10	5.4
Total	4.28	11.09	12.21	12.22	99.7

Table 3: Percentage of DNA sequences identified as either retroelements or DNA transposons, and total interspersed repeats. Observed values for the entire *T. cacao* genome, for all recombination hotspots (HS), and ubiquitous hotspots (hotspots in the same location in at least eight different populations). Also presented are mean percentage of these sequences for 1000 simulations of hotspots equivalent in size and count as the ubiquitous set and the percentile at which the observed value for the ubiquitous set is found in the distribution of the simulated set (Sim).

	TSSs (500bp)	TTSs (500bp)	Exon	Intron
Amelonado	1	1	0.602	0.527
Contamana	1	1	0.000	0.000
Criollo	1	1	0.000	0.000
Curaray	1	1	0.346	0.058
Guianna	1	1	1.000	1.000
Iquitos	1	1	0.000	0.000
Maranon	1	1	0.000	0.000
Nacional	1	1	0.000	0.000
Nanay	1	1	0.027	0.237
Purus	1	1	0.004	0.000

Table 4: Proportion of simulated chromosomes that presented a lower amount of hotspots intersectig with TSSs, TTSs, exons, and introns. TSSs and TTSs are considered to be the 500bp upstream and downstream of coding regions, respectively.

Population	Mean Hotspot Size (kb)
Amelonado	6.9
Contamana	6.1
Criollo	6.1
Curaray	5.8
Guianna	8.6
Iquitos	7.0
Maranon	6.8
Nacional	6.9
Nanay	7.6
Purus	6.3
All hotspots	6.9

Table 5: Average hotspot size (in kb) for hotspots detected in each population and average for all hotspots.

Pop	Position L95	Position U95	Genome L95	Genome U95	Position Range Quotient	Genome Range Quotient
Amelonado	6.35e-10	7.67e-08	2.33e-10	3.13e-04	120.75	1.34e+06
Contamana	1.63e-06	1.34e-05	1.40e-09	2.64e-04	8.22	1.88e+05
Criollo	8.75e-04	4.31e-03	5.35e-07	1.66e-02	4.92	3.11e+04
Curaray	5.15e-06	2.63e-05	2.72e-09	2.02e-04	5.11	7.40e+04
Guianna	9.76e-06	1.26e-04	1.81e-09	2.96e-03	12.90	1.63e+06
Iquitos	3.50e-10	6.52e-08	1.58e-10	2.45e-04	186.29	1.55e+06
Maranon	1.98e-09	7.40e-07	2.31e-10	3.52e-04	373.35	1.52e+06
Nacional	4.80e-10	6.50e-08	2.76e-10	3.66e-04	135.60	1.33e+06
Nanay	1.65e-09	3.06e-07	2.06e-10	3.52e-04	185.32	1.71e+06
Purus	3.98e-08	5.24e-06	2.00e-09	6.35e-04	131.87	3.18e+05

Table 6: The median of the upper and lower bounds of the 95% Credibility Interval for the trace of estimates of r from all positions in the genome are presented for each population. The upper and lower bounds of the 95% probability interval for the median estimate of r for each population is also presented. The quotients of the upper and lower bounds for each interval point to a much larger genome-wide variation in r than per-position variation in the trace for the estimate of r.

Figures

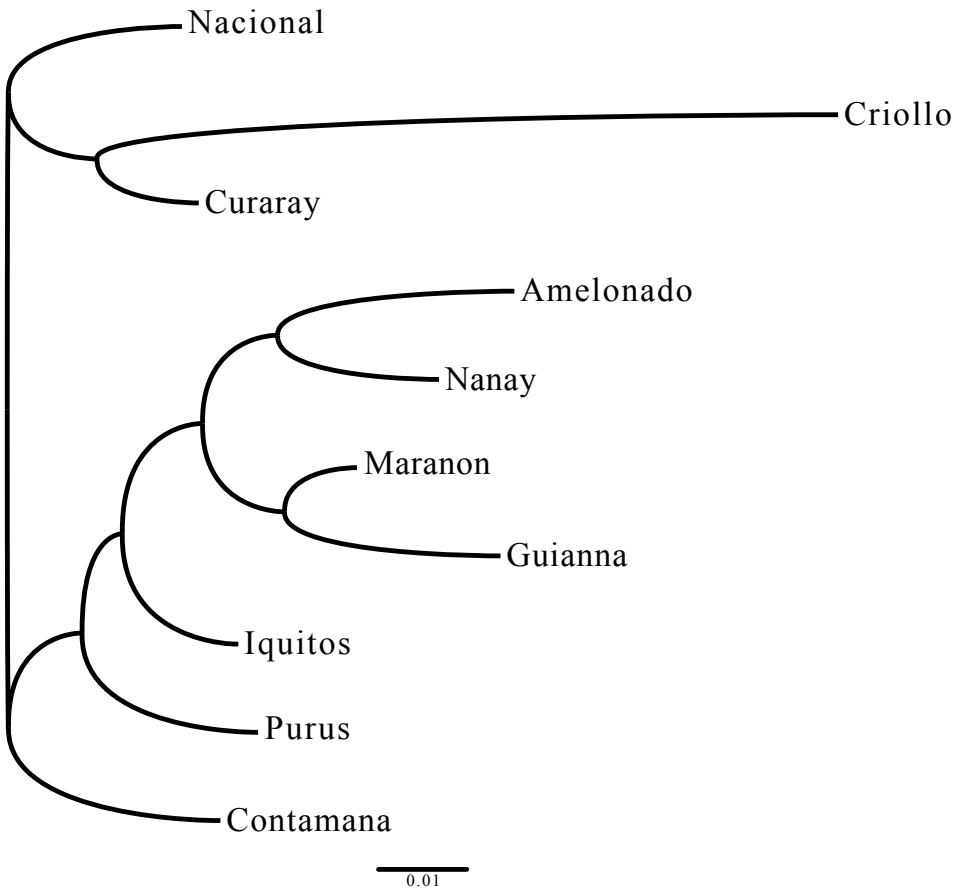

Figure 1: Drift tree for the 10 *T. cacao* populations. Modified from Cornejo et al. (2018)

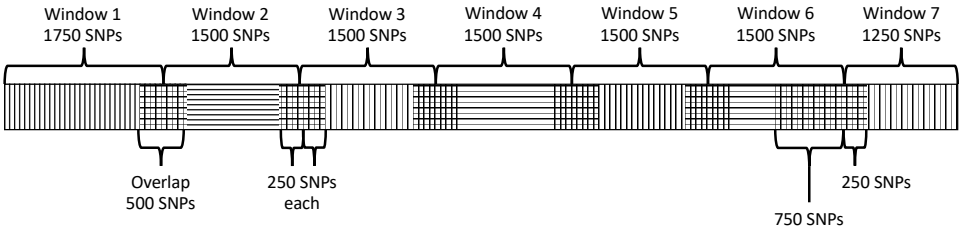

Figure 2: Example of the window layout for a 10,750 SNP chromosome. The 2,000 SNP long windows are represented by alternating horizontal and vertical lines and the overlaps between them are represented by square crosshatches. Braces above the chromosome indicate the regions from which recombination rates are extracted to generate the chromosome-wide recombination rates.

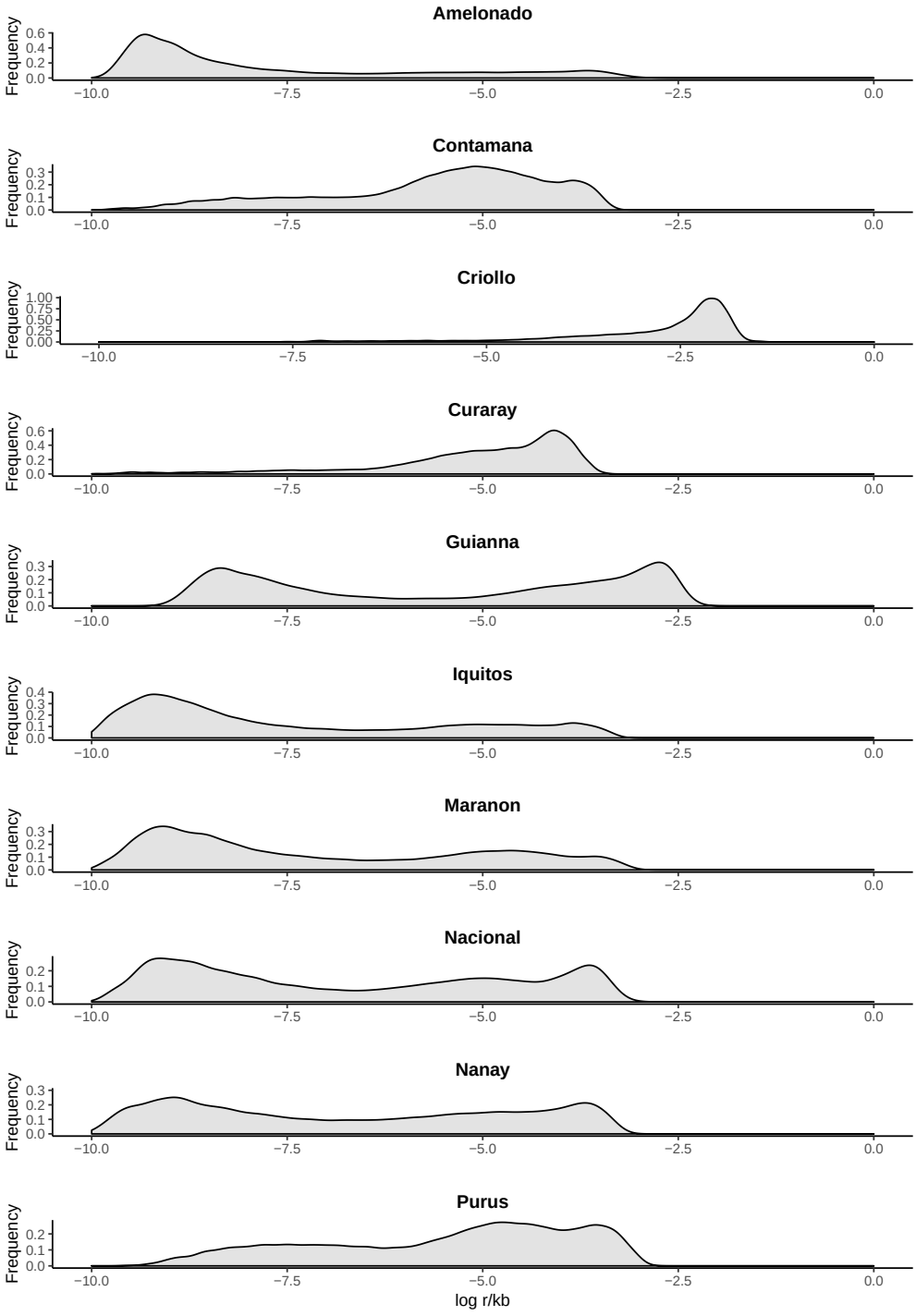

Figure 3: Distribution of log_{10} recombination rates (r/kb) along the genomes of the ten *T. cacao* populations.

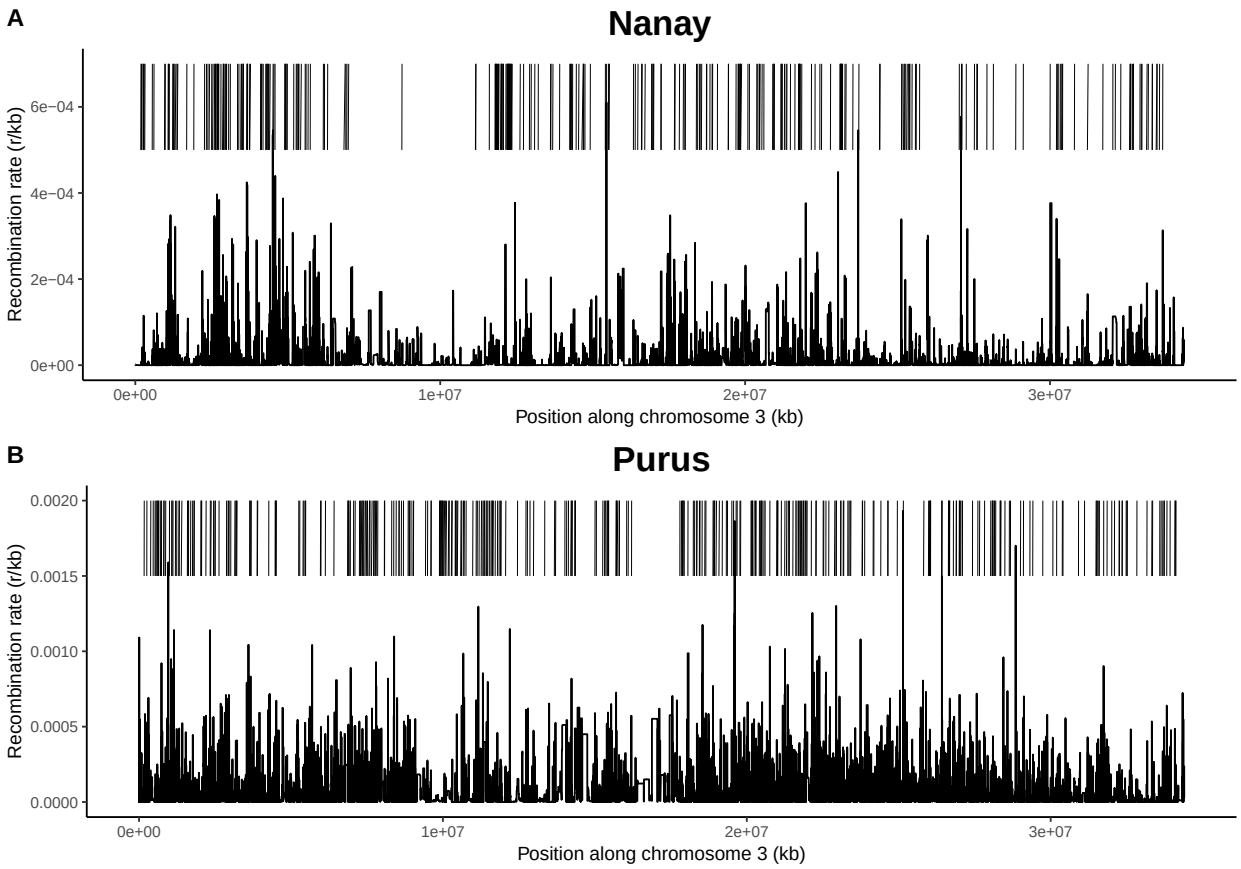

Figure 4: The third chromosomes of the Nanay (A) and Purus (B) populations were selected to exemplify the differences between populations in recombination rates (r/kb) and recombination hotspot locations (red vertical line segments).

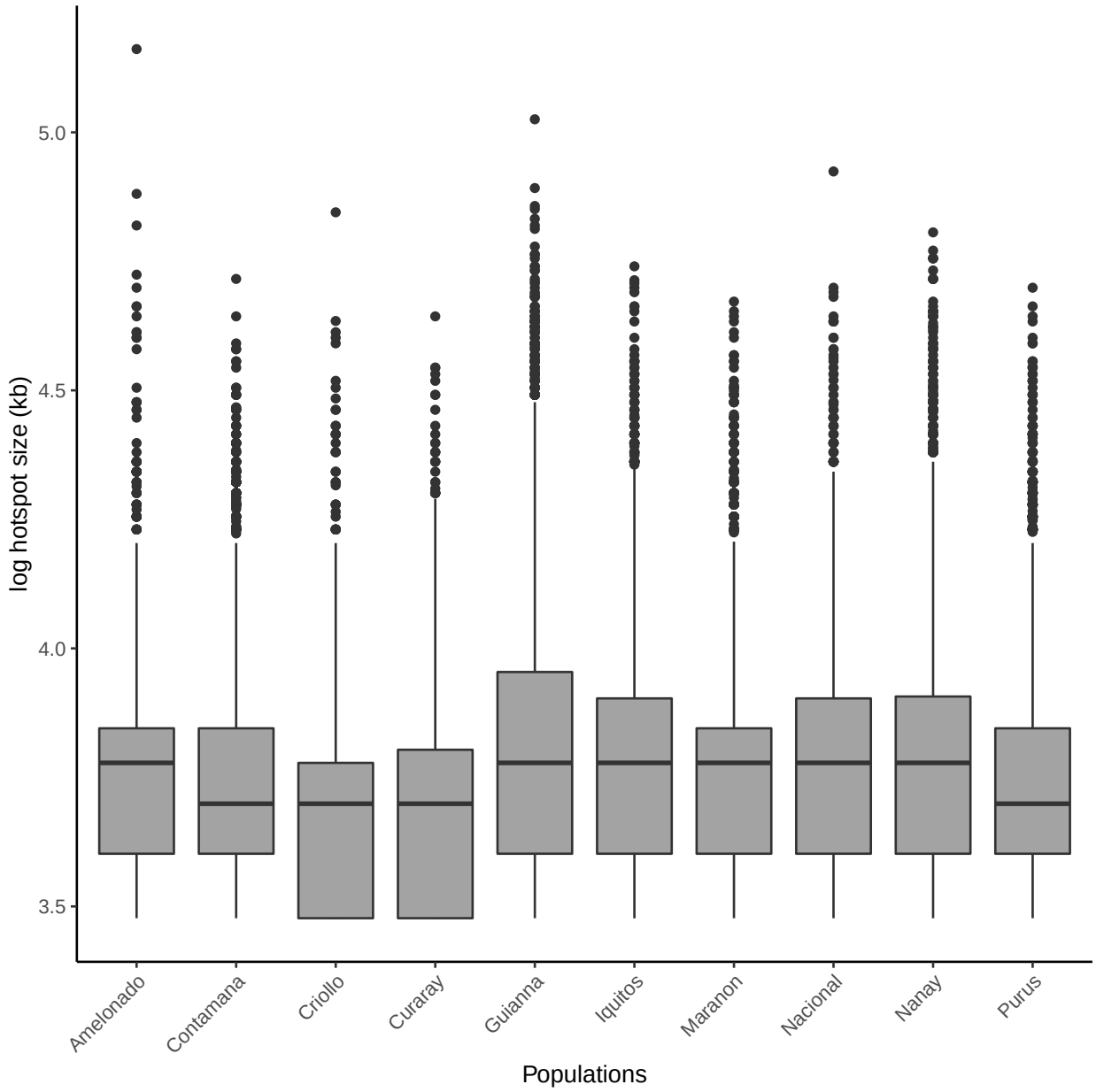

Figure 5: Boxplots of recombination hotspot sizes ($log_{10}(kb)$) by population. The horizontal line in the box represents the median value, while the points represent potential outliers.

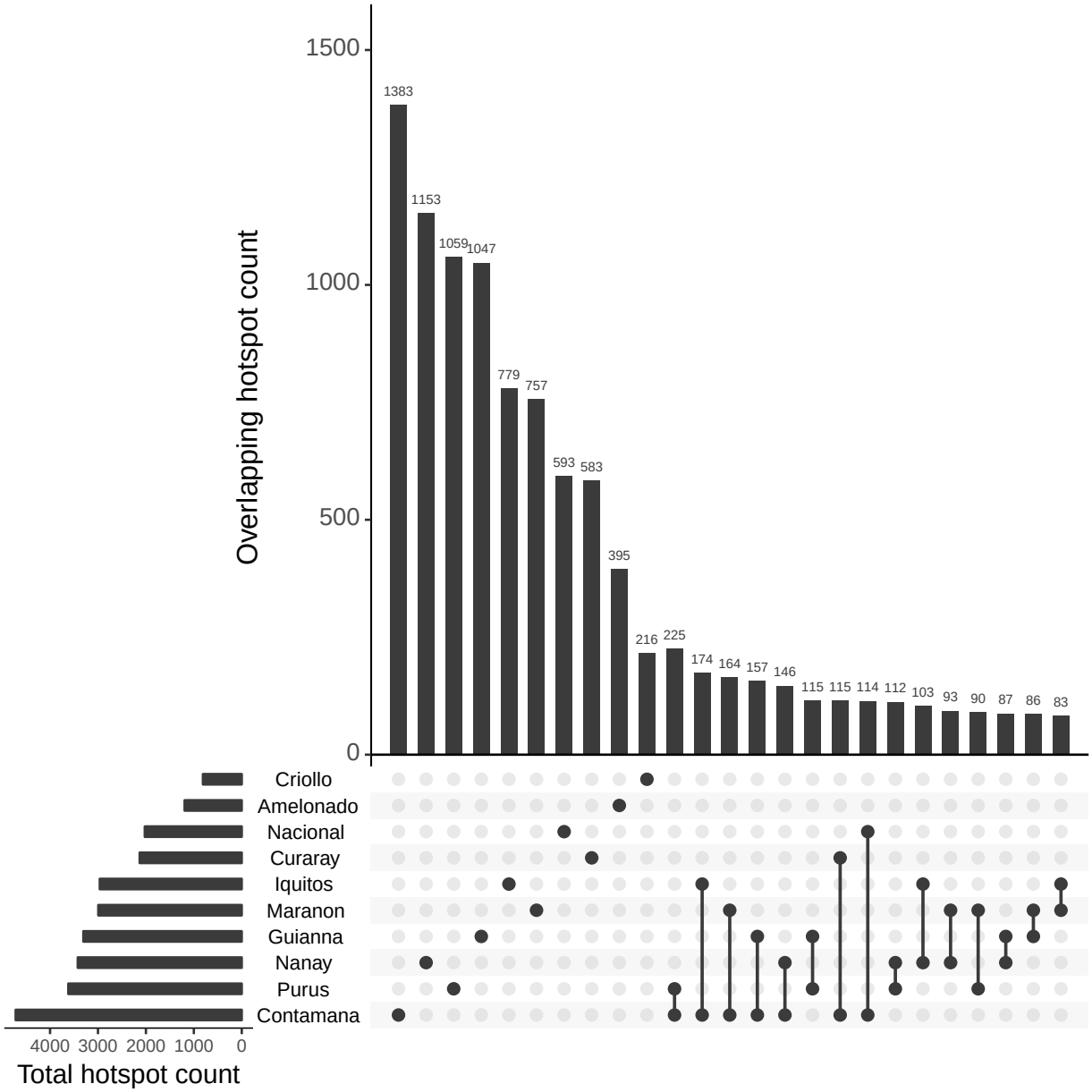

Figure 6: Upset plot showing amounts of shared hotspots. Horizontal bars represent total hotspots detected in a population, dots on the matrix represent the populations that share the hotspots represented in the vertical bar above them. The 25 largest subsets are shown.

References

Akhunov, E. D., and Coauthors, 2003: The organization and rate of evolution of wheat genomes are correlated with recombination rates along chromosome arms. *Genome research*, **13 (5)**.

Anderson, L. K., N. Salameh, H. W. Bass, L. C. Harper, W. Z. Cande, G. Weber, and S. M. Stack, 2004: Integrating genetic linkage maps with pachytene chromosome structure in maize. *Genetics*, **166 (4)**, 1923–1933, doi:10.1534/genetics.166.4.1923, URL http://www.genetics.org/content/166/4/1923, http://www.genetics.org/content/166/4/1923.full.pdf.

Auton, A., and G. McVean, 2007: Recombination rate estimation in the presence of hotspots. *Genome Research*, **17 (8)**, 1219–1227, URL http://www.ncbi.nlm.nih.gov/pmc/articles/PMC1933511/.

Auton, A., and Coauthors, 2012: A Fine-Scale Chimpanzee Genetic Map from Population Sequencing. *Science*, **336 (6078)**, 193–198, doi:10.1126/science.1216872, URL http://science.sciencemag.org/content/336/6078/193, http://science.sciencemag.org/content/336/6078/193.full.pdf.

Auton, A., and Coauthors, 2013: Genetic recombination is targeted towards gene promoter regions in dogs. *PLOS Genetics*, **9 (12)**, 1–9, doi:10.1371/journal.pgen.1003984, URL https://doi.org/10.1371/journal.pgen.1003984.

Bartley, B., 2005: *The Genetic Diversity of Cacao and Its Utilization*. CAB books, CABI, URL https://books.google.com/books?id=_I40iGVJD64C.

Begun, D. J., and C. F. Aquadro, 1992: Levels of naturally occurring dna polymorphism correlate with recombination rates in d. melanogaster. *Nature*, **356 (6369)**.

Booker, T. R., R. W. Ness, and P. D. Keightley, 2017: The recombination landscape in wild house mice inferred using population genomic data. *Genetics*, **207 (1)**, 297–309, doi:10.1534/genetics.117.300063, URL http://www.genetics.org/content/207/1/297, http://www.genetics.org/content/207/1/297.full.pdf.

Bougeard, S., and S. Dray, 2018: Supervised multiblock analysis in R with the ade4 package. *Journal of Statistical Software*, **86 (1)**, 1–17, doi:10.18637/jss.v086.i01.

Branca, A., and Coauthors, 2011: Whole-genome nucleotide diversity, recombination, and linkage disequilibrium in the model legume medicago truncatula. *Proceedings of the National Academy of Sciences*, **108 (42)**.

Brick Kevin, Smagulova Fatima, Khil Pavel, Camerini-Otero R. Daniel, and Petukhova Galina V., 2012: Genetic recombination is directed away from functional genomic elements in mice. *Nature*, **485 (7400)**, 642–645, doi:http://dx.doi.org/10.1038/nature11089, URL http://www.nature.com/nature/journal/v485/n7400/abs/nature11089.html#supplementary-information, 10.1038/nature11089.

Brunschwig, H., L. Levi, E. Ben-David, R. W. Williams, B. Yakir, and S. Shifman, 2012: Fine-scale Map of Recombination Rates and Hotspots in the Mouse Genome. *Genetics*, doi:10.1534/genetics.112.141036, URL http://www.genetics.org/content/early/2012/05/04/genetics.112.141036, http://www.genetics.org/content/early/2012/05/04/genetics.112.141036.full.pdf.

Chen, M.-M., F. Feng, X. Sui, M.-H. Li, D. Zhao, and S. Han, 2010: Construction of a framework map for pinus koraiensis sieb. et zucc. using srap, ssr and issr markers. *Trees*, **24 (4)**, 685–693, doi:10.1007/s00468-010-0438-5, URL https://doi.org/10.1007/s00468-010-0438-5.

627 Chessel, D., A.-B. Dufour, and J. Thioulouse, 2004: The ade4 package – I: One-table meth-
628 ods. *R News*, **4 (1)**, 5–10, URL https://cran.r-project.org/doc/Rnews/.

629 Choi, K., and Coauthors, 2013: *Arabidopsis* meiotic crossover hot spots overlap with
630 h2a.z nucleosomes at gene promoters. *Nature Genetics*, **45 (11)**, 1327–1336, doi:
631 10.1038/ng.2766.

632 Cornejo, O. E., and Coauthors, 2018: Population genomic analyses of the chocolate tree,
633 Theobroma cacao L., provide insights into its domestication process. *Communications*
634 *Biology*, doi:10.1038/s42003-018-0168-6.

635 Crow, J. F. J. F., 1970: (Harper international editions.). An introduction to population
636 genetics theory. Harper Row, New York.

637 Danecek Petr, and Coauthors, 2011: The variant call format and VCFtools. *Bioinformatics*,
638 **27 (15)**, 2156–2158, URL http://www.ncbi.nlm.nih.gov/pmc/articles/PMC3137218/.

639 Donnelly, P., and T. G. Kurtz, 1999: Genealogical processes for fleming-viot models with
640 selection and recombination. *Ann. Appl. Probab.*, **9 (4)**, 1091–1148, doi:10.1214/aoap/
641 1029962866, URL https://doi.org/10.1214/aoap/1029962866.

642 Dray, S., and A.-B. Dufour, 2007: The ade4 package: Implementing the duality diagram for
643 ecologists. *Journal of Statistical Software*, **22 (4)**, 1–20, doi:10.18637/jss.v022.i04.

644 Dray, S., A.-B. Dufour, and D. Chessel, 2007: The ade4 package – II: Two-table and K-table
645 methods. *R News*, **7 (2)**, 47–52, URL https://cran.r-project.org/doc/Rnews/.

646 Drost, H.-G., 2018: *philentropy: Similarity and Distance Quantification Between Probabil-*
647 *ity Functions*. URL https://CRAN.R-project.org/package=philentropy, r package version
648 0.2.0.

649 Exposito-Alonso, M., and Coauthors, 2018: The rate and potential relevance of new mu-
650 tations in a colonizing plant lineage. *PLOS Genetics*, **14 (2)**, 1–21, doi:10.1371/journal.
651 pgen.1007155, URL https://doi.org/10.1371/journal.pgen.1007155.

652 Eyre-Walker, A., and P. D. Keightley, 2007: The distribution of fitness effects of new muta-
653 tions. *Nature Reviews Genetics*, **8 (8)**.

654 Felsenstein, J., 1974: The evolutionary advantage of recombination. *Genetics*, **78 (2)**,
655 737–756, URL http://www.genetics.org/content/78/2/737, http://www.genetics.org/
656 content/78/2/737.full.pdf.

657 Fernandes, J. B., M. Séguéla-Arnaud, C. Larchevêque, A. H. Lloyd, and R. Mercier, 2018:
658 Unleashing meiotic crossovers in hybrid plants. *Proceedings of the National Academy of Sci-*
659 *ences*, **115 (10)**, 2431–2436, doi:10.1073/pnas.1713078114, URL http://www.pnas.org/
660 content/115/10/2431, http://www.pnas.org/content/115/10/2431.full.pdf.

661 Goolsby, E. W., J. Bruggeman, and C. Ane, 2016: *Rphylopars: Phylogenetic Comparative*
662 *Tools for Missing Data and Within-Species Variation*. URL https://CRAN.R-project.org/
663 package=Rphylopars, r package version 0.2.9.

664 Gore, M. A., and Coauthors, 2009: A first-generation haplotype map of maize. *Science*,
665 **326 (5956)**, 1115–1117, doi:10.1126/science.1177837, URL http://science.sciencemag.
666 org/content/326/5956/1115, http://science.sciencemag.org/content/326/5956/1115.full.
667 pdf.

668 Haldane, J. B. S., 1937: The effect of variation on fitness. *The American Naturalist*, **71 (735)**,
669 337–349, URL http://www.jstor.org/stable/2457289.

670 Hellsten, U., and Coauthors, 2013: Fine-scale variation in meiotic recombination in
671 *Mimulus* inferred from population shotgun sequencing. *PNAS*, **110 (48)**, 19 478–19 482,
672 doi:10.1073/pnas.1319032110.

673 Henderson, J. S., R. A. Joyce, G. R. Hall, W. J. Hurst, and P. E. McGovern, 2007: Chemical
674 and archaeological evidence for the earliest cacao beverages. *Proceedings of the National*
675 *Academy of Sciences*, **104 (48)**, 18 937–18 940, doi:10.1073/pnas.0708815104, URL http:
676 //www.pnas.org/content/104/48/18937.abstract, http://www.pnas.org/content/104/48/
677 18937.full.pdf.

678 Hudson, R. R., and N. L. Kaplan, 1988: The coalescent process in models with selection and
679 recombination. *Genetics*, **120 (3)**, 831–840, URL http://www.genetics.org/content/120/
680 3/831, http://www.genetics.org/content/120/3/831.full.pdf.

681 Kim, S., and Coauthors, 2007: Recombination and linkage disequilibrium in arabidopsis
682 thaliana. *Nature Genetics*, **39 (9)**.

683 Kosambi, D. D., 1943: The estimation of map distances from recombination val-
684 ues. *Annals of Eugenics*, **12 (1)**, 172–175, doi:10.1111/j.1469-1809.1943.tb02321.x,
685 URL https://onlinelibrary.wiley.com/doi/abs/10.1111/j.1469-1809.1943.tb02321.x, https:
686 //onlinelibrary.wiley.com/doi/pdf/10.1111/j.1469-1809.1943.tb02321.x.

687 Kundu, A., A. Chakraborty, N. A. Mandal, D. Das, P. G. Karmakar, N. K. Singh, and
688 D. Sarkar, 2015: A restriction-site-associated dna (rad) linkage map, comparative genomics
689 and identification of qtl for histological fibre content coincident with those for retted
690 bast fibre yield and its major components in jute (corchorus olitorius l., malvaceae s. l.).
691 *Molecular Breeding*, **35 (1)**, 19, doi:10.1007/s11032-015-0249-x, URL https://doi.org/10.
692 1007/s11032-015-0249-x.

693 Lê, S., J. Josse, and F. Husson, 2008: FactoMineR: A package for multivariate analysis.
694 *Journal of Statistical Software*, **25 (1)**, 1–18, doi:10.18637/jss.v025.i01.

695 Li, W. H., and M. Nei, 1974: Stable linkage disequilibrium without epistasis in subdivided
696 populations. *Theoretical population biology.*, **6 (2)**, 173–183.

Lynch, M., 2010: Evolution of the mutation rate. *Trends in genetics : TIG*, **26 (8)**, 345–352, URL http://www.ncbi.nlm.nih.gov/pmc/articles/PMC2910838/.

Martinez-perez, E., M. Schvarzstein, C. Barroso, J. M. Lightfoot, A. F. Dernburg, and A. M. Villeneuve, 2008: Crossovers trigger a remodeling of meiotic chromosome axis composition that is linked to two-step loss of sister chromatid cohesion. *Genes & development*, **22 20**, 2886–901.

Mcvean, G., 2010: What drives recombination hotspots to repeat dna in humans? *Philosophical Transactions of the Royal Society B*, **365 (1544)**, 1213–1218.

McVean, G. A. T., S. R. Myers, S. Hunt, P. Deloukas, D. R. Bentley, and P. Donnelly, 2004: The fine-scale structure of recombination rate variation in the human genome. *Science*, **304 (5670)**, 581–584, doi:10.1126/science.1092500, URL http://science.sciencemag.org/content/304/5670/581, http://science.sciencemag.org/content/304/5670/581.full.pdf.

Mézard, C., 2006: Meiotic recombination hotspots in plants. *Biochemical Society Transactions*, **34 (4)**, 531–534, doi:10.1042/BST0340531, URL http://www.biochemsoctrans.org/content/34/4/531, http://www.biochemsoctrans.org/content/34/4/531.full.pdf.

Motamayor, J. C., P. Lachenaud, da Silva e Mota Jay Wallace, R. Loor, D. N. Kuhn, S. J. Brown, and R. J. Schnell, 2008: Geographic and Genetic Population Differentiation of the Amazonian Chocolate Tree (Theobroma cacao L). *PLOS ONE*, **3 (10)**, e3311, doi:https://doi.org/10.1371/journal.pone.0003311.

Motamayor, J. C., and Coauthors, 2013: The genome sequence of the most widely cultivated cacao type and its use to identify candidate genes regulating pod color. *Genome Biology*, **14 (6)**, r53, doi:10.1186/gb-2013-14-6-r53, URL https://doi.org/10.1186/gb-2013-14-6-r53.

Myers, S., L. Bottolo, C. Freeman, G. McVean, and P. Donnelly, 2005: A Fine-Scale Map of Recombination Rates and Hotspots Across the Human Genome. *Science*, **310 (5746)**, 321–324, doi:10.1126/science.1117196, URL http://science.sciencemag.org/content/310/5746/321, http://science.sciencemag.org/content/310/5746/321.full.pdf.

Ohta, T., 1982: Linkage disequilibrium due to random genetic drift in finite subdivided populations. *Proceedings of the National Academy of Sciences*, **79 (6)**, 1940–1944, doi:10.1073/pnas.79.6.1940, URL http://www.pnas.org/content/79/6/1940, http://www.pnas.org/content/79/6/1940.full.pdf.

Paape, T., P. Zhou, A. Branca, R. Briskine, N. Young, and P. Tiffin, 2012: Fine-Scale Population Recombination Rates, Hotspots, and Correlates of Recombination in the Medicago truncatula Genome. *Genome Biology and Evolution*, **4 (5)**, 726–737, URL http://www.ncbi.nlm.nih.gov/pmc/articles/PMC3381680/.

Quinlan, A. R., and I. M. Hall, 2010: Bedtools: a flexible suite of utilities for comparing genomic features. *Bioinformatics*, **26 (6)**, 841–842, doi:10.1093/bioinformatics/btq033, URL +http://dx.doi.org/10.1093/bioinformatics/btq033, /oup/backfile/content_public/journal/bioinformatics/26/6/10.1093_bioinformatics_btq033/3/btq033.pdf.

R Core Team, 2018: *R: A Language and Environment for Statistical Computing*. Vienna, Austria, R Foundation for Statistical Computing, URL https://www.R-project.org/.

Revelle, W., 2018: *psych: Procedures for Psychological, Psychometric, and Personality Research*. Evanston, Illinois, Northwestern University, URL https://CRAN.R-project.org/package=psych, r package version 1.8.10.

Rizzon, C., G. Marais, M. Gouy, and C. Biémont, 2002: Recombination rate and the distribution of transposable elements in the drosophila melanogaster genome. *Genome Research*,

12 (3), 400–407, doi:10.1101/gr.210802, URL http://genome.cshlp.org/content/12/3/400.abstract, http://genome.cshlp.org/content/12/3/400.full.pdf+html.

Rodgers, K., and M. Mcvey, 2015: Error-prone repair of dna double-strand breaks. *Journal of Cellular Physiology*, **231**.

Ross-Ibarra, J., 2004: The Evolution of Recombination under Domestication: A Test of Two Hypotheses. *The American Naturalist*, **163 (1)**, 105–112, doi:10.1086/380606, URL https://doi.org/10.1086/380606, pMID: 14767840, https://doi.org/10.1086/380606.

Sanjuán, R., A. Moya, and S. F. Elena, 2004: The distribution of fitness effects caused by single-nucleotide substitutions in an rna virus. *Proceedings of the National Academy of Sciences*, **101 (22)**, 8396–8401, doi:10.1073/pnas.0400146101, URL http://www.pnas.org/content/101/22/8396, http://www.pnas.org/content/101/22/8396.full.pdf.

Schnable, P. S., and Coauthors, 2009: The b73 maize genome: complexity, diversity, and dynamics. *Science (New York, N.Y.)*, **326 (5956)**.

Shanfelter, A., S. L. Archambeault, and M. A. White, 2018: Fine-scale recombination landscapes between a freshwater and marine population of threespine stickleback fish. *bioRxiv*, doi:10.1101/430249, URL https://www.biorxiv.org/content/early/2018/09/29/430249, https://www.biorxiv.org/content/early/2018/09/29/430249.full.pdf.

Singhal, S., and Coauthors, 2015: Stable recombination hotspots in birds. *Science*, **350 (6263)**, 928–932, doi:10.1126/science.aad0843, URL http://science.sciencemag.org/content/350/6263/928, http://science.sciencemag.org/content/350/6263/928.full.pdf.

Siol, M., I. Bonnin, I. Oliveri, J. M. Prosperi, and J. Ronfort, 2007: Effective population size associated with self-fertilization: lessons from temporal changes in allele frequencies in the selfing annual medicago truncatula. *Journal of Evolutionary Biology*, **20 (6)**, 2349–2360, doi:10.1111/j.1420-9101.2007.01409.x, URL https://onlinelibrary.wiley.com/doi/

767 abs/10.1111/j.1420-9101.2007.01409.x, https://onlinelibrary.wiley.com/doi/pdf/10.1111/
768 j.1420-9101.2007.01409.x.

769 Smith, A., R. Hubley, and P. Green, 2016: Repeatmasker open-4.0.(2013-2015).

770 Stapley, J., P. G. D. Feulner, S. E. Johnston, A. W. Santure, and C. M. Smadja, 2017: Vari-
771 ation in recombination frequency and distribution across eukaryotes: patterns and pro-
772 cesses. *Philosophical Transactions of the Royal Society B: Biological Sciences*, **372 (1736)**,
773 doi:10.1098/rstb.2016.0455, URL http://rstb.royalsocietypublishing.org/content/372/
774 1736/20160455, http://rstb.royalsocietypublishing.org/content/372/1736/20160455.full.
775 pdf.

776 Stevison, L. S., and Coauthors, 2016: The time scale of recombination rate evolution in great
777 apes. *Molecular Biology and Evolution*, **33 (4)**, 928–945, doi:10.1093/molbev/msv331.

778 Wloch, D. M., K. Szafraniec, R. H. Borts, and R. Korona, 2001: Direct estimate of the
779 mutation rate and the distribution of fitness effects in the yeast saccharomyces cerevisiae.
780 *Genetics*, **159 (2)**, 441–452, URL http://www.genetics.org/content/159/2/441, http://
781 www.genetics.org/content/159/2/441.full.pdf.

782 Wu, J., and Coauthors, 2003: Physical maps and recombination frequency of six rice chro-
783 mosomes. *Plant Journal*, **36 (5)**, 720–730.

784 Yelina, N., P. Diaz, C. Lambing, and I. R. Henderson, 2015: Epigenetic control of
785 meiotic recombination in plants. *Science China Life Sciences*, **58 (3)**, 223–231, doi:
786 10.1007/s11427-015-4811-x, URL https://doi.org/10.1007/s11427-015-4811-x.